CALAMITY
Calamity: A Journal of Disaster Technology and Engineering
CALAMITY 4(1): 53–68
ISSN 3025-4140

Institute for Advanced Science, Social and Sustainable Future
MORALITY BEFORE KNOWLEDGE

Politicized hydrology: Spatial associations among tree-cover loss, protected forests, and hydrometeorological disaster exposure

Miftahul Ardli[1,*]
[1] *Department of Environmental Science, Graduate School of Sustainable Development, Universitas Indonesia, Central Jakarta, Special Capital Region of Jakarta 10430, Indonesia.*
*Correspondence: mifardli21@gmail.com

Received Date: January 17, 2026 Revised Date: May 16, 2026 Accepted Date: July 29, 2026

ABSTRACT

Background: Sumatra has experienced increasing hydrometeorological disaster pressure, particularly floods and landslides, in areas connected to upstream watershed degradation and spatial governance problems. This study examines how disaster distribution, forest conversion discourse, and spatial planning governance interact in shaping flood and landslide risk along the Bukit Barisan corridor. **Methods**: Using a secondary-data based qualitative-spatial approach, this study analyzes the BIG-BNPB 2025 spatial disaster dataset obtained from the Tanah Air Indonesia geoportal and interprets it through policy documents and scientific literature on watershed degradation, environmental governance, and political ecology. **Findings:** The results show that hydrometeorological disaster areas are spatially concentrated in Aceh, North Sumatra, and West Sumatra. Based on the compiled disaster polygons, flood areas dominate the observed disaster distribution, reaching approximately 3,980.56 km^2, while landslide and landslide-prone areas account for approximately 136.95 km^2 and 556.90 km^2, respectively. Aceh records the largest total disaster-affected area, reaching approximately 3.119.48 km^2, indicating a strong concentration of flood risk within upstream-downstream watershed systems. **Conclusion**: These findings suggest that flood risk in Sumatra should not be interpreted solely as a rainfall-driven natural phenomenon, but also as a governance-related risk amplified by reduced watershed carrying capacity, sedimentation, and weakened ecological control in spatial planning. **Novelty/Originality of this article:** This study argues that hydrometeorological disasters in Sumatra represent institutionally produced risks when legal and policy instruments fail to protect upstream ecological functions. Strengthening watershed-based policy audits, ecological licensing governance, and stricter control of upstream land conversion is therefore essential for long-term flood and landslide mitigation in Sumatra.

KEYWORDS: deforestation; disaster mitigation; flood risk; political ecology; watershed degradation.

1. Introduction

Aceh, North Sumatra, and West Sumatra combine steep sections of the Bukit Barisan mountain chain with densely settled downstream plains and coastal corridors. This geomorphological configuration creates short upstream–downstream connections through which intense rainfall, slope disturbance, sediment movement, channel capacity, and floodplain occupation can interact. Disaster risk in these provinces therefore cannot be

Cite This Article:
Ardli, M. (2026). Politicized hydrology: Spatial associations among tree-cover loss, protected forests, and hydrometeorological disaster exposure. *Calamity: A Journal of Disaster Technology and Engineering, 4*(1), 53-68. https://doi.org/10.61511/calamity.v4i1.2026.3863

reduced to rainfall alone; it emerges from the interaction of physical hazards, exposure, land-cover conditions, and institutional decisions governing land and water.

Forest hydrology research has long shown that forest disturbance can alter infiltration, soil protection, runoff generation, and sediment delivery, although the magnitude and direction of effects depend on catchment characteristics and event scale (Bruijnzeel, 2004; Bradshaw et al., 2007; Tan-Soo et al., 2016). In Indonesia, landscape-level land-use change has also been associated with changing flood responses (Tarigan, 2016). These findings support closer examination of tree-cover loss around mapped hazard areas, while cautioning against treating spatial co-occurrence as proof of a complete rainfall–runoff causal chain.

Contemporary flood-risk assessment increasingly integrates remote sensing, geographic information systems (GIS), hydrological variables, and data-driven models. Recent reviews emphasize that reliable susceptibility mapping normally combines terrain, drainage, rainfall, land cover, and event inventories, with validation appropriate to the intended decision scale (Islam et al., 2025). Machine-learning and process-informed frameworks can improve predictive capability, but their transferability depends on meaningful physical features and watershed context (Avand et al., 2021; Pakdehi et al., 2024). In data-limited settings, transparent spatial screening remains useful when its evidentiary limits are explicitly stated.

A second gap concerns governance. Political ecology and environmental-governance research shows that the distribution of environmental risk is influenced by authority, territorial control, legal classification, and institutional fit across ecological boundaries (Robbins, 2012; Ostrom, 2009; Peluso & Lund, 2011; Kelly & Peluso, 2015; Young, 2017). However, disaster inventories are often analyzed separately from remote-sensing indicators and legal forest-status information. The concept of politicized hydrology is used here as an interpretive framework: hydrological risk is understood as physically produced but institutionally mediated through land-use and forest-estate decisions.

Tree-cover loss was selected as an environmental-pressure indicator because it is measurable consistently across provincial boundaries and because forest disturbance can affect several components of watershed functioning. Canopy removal can reduce interception, while associated ground disturbance can change infiltration, soil protection, and sediment delivery. These mechanisms are well established conceptually, but their magnitude varies with soil, slope, land management, regrowth, drainage infrastructure, and storm characteristics (Bruijnzeel, 2004). At the same time, Hansen loss is a remotely sensed canopy-change signal rather than a legal or ecological classification of deforestation. A detected loss pixel may represent permanent conversion, plantation harvesting, fire, storm damage, or other canopy-removal processes. The study therefore uses the term tree-cover loss deliberately and avoids assigning a specific driver to individual pixels without supporting land-use or permit data.

This caution is especially important in Indonesia, where forest loss is produced by heterogeneous and shifting land-use processes. Previous national-scale research has identified contributions from industrial timber and fiber plantations, oil-palm expansion, mining, smallholder activities, fire, and other transitions, with the relative importance of drivers changing across locations and periods (Abood et al., 2015; Austin et al., 2017; Austin et al., 2019; Gaveau et al., 2022). Political-economic research also shows that institutional incentives and jurisdictional arrangements can influence deforestation outcomes, demonstrating why land-cover change cannot be interpreted independently of governance (Burgess et al., 2012). These studies motivate the governance component of the present analysis, but they do not justify attributing the observed loss in Aceh, North Sumatra, or West Sumatra to any single industry or political process.

The legal status of forest land adds a second spatial dimension. Indonesia's forest estate is governed through formal categories that differentiate protection, conservation, and production functions. These categories matter because they establish different management objectives and constraints, yet a legal designation is not itself a direct measure of current canopy condition or management effectiveness. Research on land governance in tropical regions emphasizes that formal rules interact with markets, administrative authority, enforcement capacity, and cross-scale institutional arrangements (Lemos & Agrawal, 2006; Lambin et al., 2014). More broadly, land-use transitions can be driven by pressures that operate beyond local administrative boundaries (Lambin & Meyfroidt, 2011). Overlaying tree-cover loss with legally established forest functions can therefore identify where additional monitoring is warranted, while remaining distinct from a permit audit or determination of illegality.

Accordingly, the study treats politicized hydrology as an analytical bridge rather than a causal label. The hydrological component concerns measurable spatial patterns of mapped hazard footprints and land-cover change; the political component concerns the legal and institutional arrangements through which land and forest functions are allocated, monitored, and enforced. Political ecology provides a vocabulary for examining how access, territorial control, and formalization shape environmental outcomes (Peluso & Lund, 2011; Kelly & Peluso, 2015; Robbins, 2012), while environmental-governance scholarship stresses the difficulty of matching institutions to ecological processes that cross scales and jurisdictions (Ostrom, 2009; Biermann et al., 2012; Young, 2017). The empirical contribution here is deliberately narrower: it quantifies spatial co-occurrence and identifies monitoring priorities that can be examined more directly in subsequent hydrological, licensing, and field-based research.

This study addresses these gaps by integrating three evidence layers within the defined study area: (1) 65 mapped flood, landslide, and landslide-area polygons; (2) annual and cumulative Hansen tree-cover loss for 2014–2024; and (3) legally established forest-function polygons from the BIG One Map service. The objectives were to: (i) quantify the distribution of mapped hydrometeorological disaster areas; (ii) measure regional and polygon-level tree-cover loss; (iii) assess tree-cover loss within Protection Forest, conservation, and production forest functions; and (iv) interpret the results for monitoring, watershed governance, and disaster-risk reduction without claiming direct causality.

2. Methods

2.1 Study area and disaster-polygon dataset

The study covered Aceh, North Sumatra, and West Sumatra. The primary spatial inventory was the BIG Peta Area Terdampak Bencana Hidrometeorologi dataset dated 31 January 2026 (Badan Informasi Geospasial, 2026). Geospatial Information Agency (*Badan Informasi Geospasial*/BIG) delineated the mapped areas from PlanetScope and RapidEye basemap imagery acquired during October, November, and December 2025. The basemap source imagery had a 4.77 m pixel size and was supplied in WGS 84 Web Mercator (EPSG:3857), whereas the distributed vector shapefile is stored in WGS 84 geographic coordinates (EPSG:4326). Interpretation was conducted at approximately 1:12.500, with a reported horizontal positional accuracy of ±10–15 m. The vector inventory contains 65 polygons classified as flood (*Banjir*), landslide (*Longsor*), or landslide area (*Area Longsor*). BIG describes Area Longsor as an area where several landslide occurrences were mapped; it is therefore treated as an affected-area class rather than a generic susceptibility zone. The source attributes include province, regency/city, and area in square kilometres. The official source-area field was retained rather than recomputed, and BIG notes that the image-based delineations had not been field-verified.

2.2 Tree-cover-loss extraction

Tree-cover loss was extracted from UMD Hansen Global Forest Change 2025 v1.13 in Google Earth Engine. The treecover2000 band was used to define baseline tree cover, with pixels retained when canopy cover was at least 30%. The lossyear band identified annual loss from 2014 through 2024, a period preceding the late-2025 disaster-image interpretation. Pixel area was calculated using ee.Image.pixelArea, converted to hectares, and reduced at a nominal 30 m scale. Outputs were generated for each province and each of the 65 disaster-affected polygons. Hansen loss is interpreted as gross tree-cover loss and not automatically as permanent deforestation (Hansen et al., 2013).

The temporal ordering of the datasets was chosen to reduce one common ambiguity in post-disaster land-cover analysis. Tree-cover loss was summarized for 2014–2024, whereas the disaster-affected polygons were interpreted from imagery acquired in October–December 2025 and released by BIG in January 2026. Thus, the loss period precedes the mapped disaster footprints. This ordering does not establish that earlier loss caused the 2025 hazards, because the analysis lacks event rainfall, runoff routing, and disturbance timing at sub-annual resolution. It does, however, make the tree-cover metric interpretable as a pre-event landscape-history indicator rather than as a canopy-change response to the mapped late-2025 disasters.

Three complementary loss metrics were retained because each answers a different screening question. Absolute loss in hectares measures the amount of canopy loss intersecting a reporting unit and is useful for identifying large concentrations of change. Proportional loss divides loss by the year-2000 tree-cover baseline within the same unit and therefore reduces, but does not eliminate, the influence of polygon size. Weighted loss at the hazard-class level was calculated from summed loss divided by summed baseline tree cover, whereas the reported median proportional loss describes the typical polygon without allowing very large polygons to dominate the summary. These distinctions are necessary because a large flood footprint may contain a high absolute loss even when its relative loss is moderate.

2.3 Legally established forest areas

Legal forest-function information was obtained from the BIG Kebijakan Satu Peta ArcGIS REST service, layer "Forest-Estate Designation (*Penetapan Kawasan Hutan*)," whose service metadata was published on 8 August 2024 (Badan Informasi Geospasial, 2024). The polygon layer uses EPSG:4326 and corresponds to the final stage of forest-estate gazettement at a nominal scale of 1:50,000. The FUNGSITAP attribute was decoded using the official geospatial data standard of the Ministry of Environment and Forestry, as stipulated in Decree of the Minister of Environment and Forestry Number 398 of 2024/*Keputusan Menteri Lingkungan Hidup dan Kehutanan Nomor 398 Tahun 2024*. Functions were grouped as Protection Forest; conservation areas (including nature reserves, wildlife sanctuaries, national parks, nature recreation parks, hunting parks, and grand forest parks, including marine subtypes); production forests (HP, HPT, and HPK); and water bodies. This grouping was interpreted in accordance with the national regulatory framework governing forest planning and changes in forest status and function, as set out in Regulation of the Minister of Environment and Forestry Number 7 of 2021/*Peraturan Menteri Lingkungan Hidup dan Kehutanan Nomor 7 Tahun 2021*. Hansen baseline and loss area were calculated for 354 decoded source polygons. Of these, 289 represented the forest functions reported in Table 4, and 65 were water-body records excluded from the forest-function comparison. Grouped forest-function polygon sums were used as screening totals; however, potential overlaps or inconsistencies in the source layer remain a limitation.

The forest-function overlay was interpreted with similar caution. The analysis summarizes Hansen baseline tree cover and 2014–2024 loss inside source polygons classified by official forest function. Because forest-estate polygons are legal-geographic objects rather than independently mapped ecological stands, the resulting values indicate canopy conditions within those legal units. They should not be read as estimates of unlawful clearing. In addition, the source layer can contain multipart geometries, adjacent units, or potential overlaps that affect grouped sums. For this reason, the analysis reports the number of source polygons and explicitly treats the aggregated values as screening totals, to be followed by geometry-level and document-level verification when decisions or enforcement actions are contemplated.

Processing and quality checks were completed in Google Earth Engine and Python 3.11 using pandas, GeoPandas, SciPy, and Matplotlib. Source totals were reconciled against the 65-polygon inventory; annual provincial loss was checked against cumulative totals; and feature counts were verified after each overlay. Descriptive statistics were summarized by province, hazard class, and forest function. Spearman rank correlation tested the association between mapped-polygon area and (a) absolute overlapping tree-cover loss and (b) proportional loss relative to baseline tree cover. A Kruskal–Wallis test assessed whether proportional loss differed among the three mapped classes. Statistical significance was evaluated at $\alpha = 0.05$. Because larger polygons mechanically contain more pixels, the absolute-loss correlation was interpreted primarily as a scale- and co-location diagnostic rather than as causal validation.

The statistical tests were selected to match the exploratory nature of the data. Spearman rank correlation does not assume a linear relationship or normally distributed variables and is therefore appropriate for highly skewed polygon areas and loss values. The first test asks whether larger mapped polygons tend to contain more absolute loss; because a geometric size effect is expected, the coefficient is interpreted as a co-location and scale diagnostic. The second test uses proportional loss to ask whether larger polygons also tend to have systematically higher loss relative to baseline. The Kruskal–Wallis test then compares proportional-loss distributions among flood, landslide, and landslide-area polygons without assuming normal distributions. No test in this design identifies a rainfall–runoff mechanism or estimates the causal effect of tree-cover loss on the occurrence of floods or landslides.

The governance interpretation was limited to official forest-function classifications, applicable geospatial standards, and peer-reviewed literature. No systematic coding of regional spatial plans, licensing files, or court records was conducted. The analysis did not include event-specific rainfall, digital elevation models, river-basin routing, hydrodynamic simulation, population or asset exposure, or ground truthing. The BIG classes also differ geometrically: a Longsor polygon represents a mapped landslide area, whereas an Area Longsor polygon aggregates an area containing several mapped landslide occurrences. Accordingly, the study evaluates spatial association and screening-level indicators, not the causal effect of tree-cover loss on a particular flood or landslide event and not a complete disaster-risk assessment.

3. Results and Discussion

3.1 Distribution of mapped hydrometeorological disaster areas

The inventory contains 38 flood polygons, 17 landslide polygons, and 10 landslide-area polygons. Their combined mapped area is 4,674.41 km^2. Floods account for 3,980.56 km^2 (85.16%), landslide areas for 556.90 km^2 (11.91%), and landslides for 136.95 km^2 (2.93%). Aceh contains 66.74% of the mapped area, followed by North Sumatra (25.04%) and West Sumatra (8.23%). Figure 1 shows the distribution of the 65 mapped polygons across the three study provinces.

Table 1. Mapped disaster-affected polygons and affected area by province and hazard class

	Aceh	North Sumatra	West Sumatra	Total
Flood (n)	17	9	12	38
Flood (km^2)	2,743.10	853.77	383.69	3,980.56
Landslide (n)	8	6	3	17
Landslide (km^2)	43.64	92.31	1.00	136.95
Landslide area (n)	6	4	0	10
Landslide area (km^2)	332.74	224.17	0.00	556.90
Total (km^2)	3,119.48	1,170.25	384.69	4,674.41

(BIG hydrometeorological disaster-affected area dataset, processed by the author)

The largest flood polygons occur in North Aceh (780.87 km²), East Aceh (518.49 km²), Langkat (481.68 km²), and Aceh Tamiang (440.61 km²). Central and South Tapanuli display a mixed pattern in which flood and slope-related polygons coexist. These concentrations identify priority areas where upstream land conditions, channel sediment, settlement exposure, and early-warning coverage should be investigated together.

The dominance of flood area should be interpreted as dominance of mapped spatial footprint, not necessarily dominance of event frequency, human exposure, or social impact. A single large flood polygon can contribute far more area than multiple small landslide polygons, while a small slope failure can still produce severe localized consequences. The inventory is therefore best read as an image-interpreted affected-area inventory rather than as a direct measure of disaster frequency, vulnerability, or impact. Its principal value for this study is that it provides a common set of geometries against which pre-event land-cover history can be summarized and locations for more detailed follow-up can be prioritized.

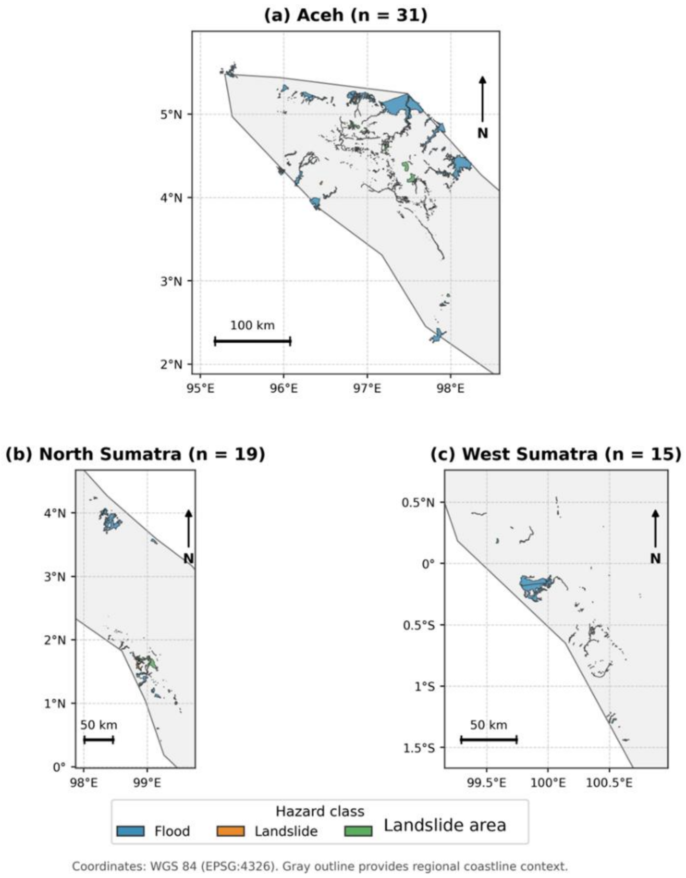

Fig. 1. Distribution of 65 mapped hydrometeorological disaster-affected polygons in (a) Aceh, (b) North Sumatra, and (c) West Sumatra. Graticules are shown in WGS 84 (EPSG:4326).

Provincial contrasts are pronounced. Aceh contributes 3,119.48 km², or 66.74% of the total mapped area, and its profile is dominated by broad flood footprints. North Sumatra contributes 1,170.25 km² and shows a more mixed pattern, with large flood areas in Langkat and South Tapanuli alongside substantial landslide and landslide-area polygons in Central and South Tapanuli. West Sumatra contributes 384.69 km², but its lower mapped area should not automatically be equated with low vulnerability, as vulnerability and impact also depend on people, assets, infrastructure, and local response capacity, none of which are measured here. These contrasts therefore describe the geometry of the mapped inventory, not comparative social or economic disaster risk among provinces.

The spatial configuration also helps explain why administrative aggregation alone is insufficient for hydrological interpretation. Water and sediment move through catchments rather than stopping at regency or provincial boundaries. Human modification of sediment flux can propagate through river systems and alter downstream channel conditions (Syvitski et al., 2005), while land-use change can interact with storage, drainage, and floodplain processes in ways that vary across catchments (Wheater & Evans, 2009). Accordingly, the large flood polygons in North Aceh, East Aceh, Aceh Tamiang, and Langkat are not treated as evidence that a particular upstream disturbance caused a particular inundation. Instead, their extent identifies places where catchment delineation, rainfall reconstruction, sediment assessment, and upstream land-cover histories would yield the greatest additional explanatory value.

3.2 Regional tree-cover loss, 2014–2024

The three-province baseline comprised 14.61 million ha of pixels with at least 30% canopy cover in 2000. Cumulative tree-cover loss during 2014–2024 reached 1,523,287 ha (15,232.87 km^2), equivalent to 10.43% of the baseline. North Sumatra recorded both the largest absolute loss (700,650 ha) and the largest proportional loss (12.09%). Aceh ranked second in absolute loss (440,335 ha), whereas West Sumatra ranked second in proportional loss (10.01%). Annual totals were highest in 2014 and remained above 109,000 ha in every year, with an increase again during 2023–2024 (Figure 2).

Table 2. Regional tree-cover baseline and cumulative loss, 2014–2024

Province	Tree-cover baseline 2000 (ha)	Loss 2014–2024 (ha)	Loss (km^2)	Loss of baseline (%)
Aceh	4,990,257	440,335	4,403.35	8.82
North Sumatra	5,794,948	700,650	7,006.50	12.09
West Sumatra	3,820,525	382,303	3,823.03	10.01
Total	14,605,729	1,523,287	15,232.87	10.43

(Hansen Global Forest Change 2025 v1.13, processed in Google Earth Engine)

These values provide a regional indicator of environmental pressure. The provincial pattern is consistent with research showing that land-cover change can alter runoff and flood susceptibility, while contemporary risk models also require terrain, rainfall, drainage, and exposure variables (Avand et al., 2021; Islam et al., 2025).

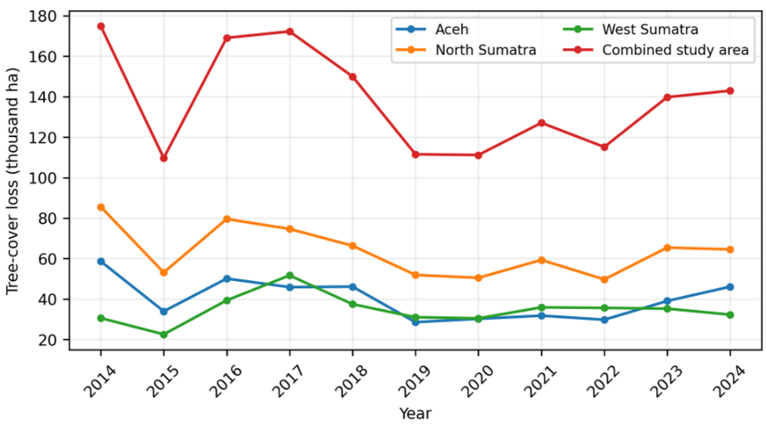

Fig. 2. Annual tree-cover loss by province and for the combined study area, 2014–2024.
(Hansen Global Forest Change 2025 v1.13, processed by the author)

Indonesia's forest-change literature reinforces why driver attribution should remain separate from the remote-sensing signal. Concession-linked logging and plantation development have historically contributed to forest loss in Indonesia (Abood et al., 2015), while the relative contribution of oil palm has changed over time and space (Austin et al., 2017). A national analysis covering 2001–2016 found multiple direct causes rather than a single dominant process throughout the study period (Austin et al., 2019), and later work documented a slowdown in deforestation associated with lower oil-palm expansion and prices during parts of the late 2010s (Gaveau et al., 2022). These findings make it inappropriate to infer the cause of the 2014–2024 pixels from the loss map alone. The present study uses those pixels to locate change, not to classify the underlying land-use transition.

The annual series is likewise descriptive rather than event-attribution evidence. The fact that combined annual loss remained above 109,000 ha in every year of the analysis and increased again in 2023–2024 indicates persistent canopy turnover across the three provinces. It does not show that any particular year produced a measurable increase in the 2025 disaster footprint. Testing such a proposition would require event-specific rainfall and discharge, spatially explicit catchment boundaries, information on the timing and location of disturbance within contributing areas, and a model capable of distinguishing land-cover effects from climate and geomorphic controls.

Nevertheless, the regional background is analytically important because the mapped 2025 disaster areas are embedded in landscapes that had already undergone substantial tree-cover change. Flood-susceptibility and flood-probability models generally require terrain, drainage, rainfall, land cover, and event information to be considered jointly (Avand et al., 2021; Islam et al., 2025). Indonesian research also illustrates that flood impacts can vary markedly across space and among affected communities (Wells et al., 2016). The regional loss totals therefore provide one antecedent landscape indicator that can be combined with hydrological and exposure variables in future catchment-scale work. Their role here is to motivate targeted follow-up, not to attribute the 2025 mapped disaster areas to a particular land-cover change.

3.3 Tree-cover loss within disaster-affected polygons and spatial association

The 65 disaster-affected polygons contained a summed 30,763 ha (307.63 km^2) of Hansen tree-cover loss, equivalent to 12.31% of their summed baseline tree cover. Flood polygons accounted for 87.53% of the summed overlapping loss, reflecting both their numerical dominance and their substantially larger spatial extent. Median proportional loss was 6.74% for flood polygons, 8.53% for landslide polygons, and 3.88% for landslide-area polygons.

Table 3. Tree-cover-loss indicators within the 65 disaster-affected polygons

Hazard class	n	Affected area (km^2)	Loss (ha)	Loss (km^2)	Median loss (%)	Weighted loss (%)
Flood	38	3,980.56	26,928	269.28	6.74	14.66
Landslide	17	136.95	1,338	13.38	8.53	12.02
Landslide area	10	556.90	2,497	24.97	3.88	4.54
Total	65	4,674.41	30,763	307.63	—	12.31

Note: sums may include spatial overlap between separately mapped hazard classes; weighted loss is loss divided by summed baseline tree cover.

(Author's analysis based on BIG and Hansen Global Forest Change data)

Mapped-polygon area was strongly correlated with absolute tree-cover loss (Spearman $\rho = 0.901$, $p < 0.001$), as expected when larger polygons contain more pixels. The correlation between polygon area and proportional loss was weaker but significant ($\rho = 0.364$, $p = 0.003$). Proportional loss did not differ significantly among the three mapped classes (Kruskal–Wallis $H = 3.19$, $p = 0.203$). These results indicate spatial co-location rather than a class-specific forest-loss signature. For flood polygons in particular, loss inside the inundated footprint should not be equated with loss in the upstream contributing catchment. The Area Longsor class likewise represents an aggregate area containing several mapped landslide occurrences rather than a single-event footprint, so its overlap statistic has a different geometric meaning from an individual landslide polygon.

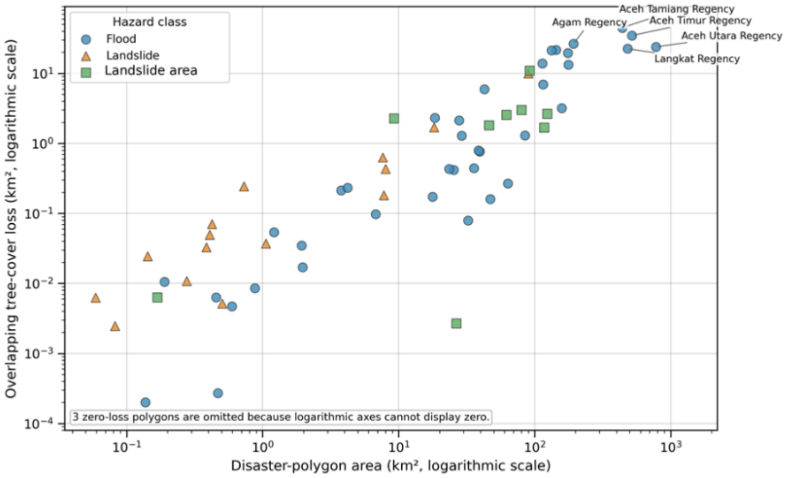

Fig. 3. Association between mapped-polygon area and tree-cover loss. Logarithmic axes exclude three zero-loss polygons; labels indicate the five polygons with the greatest absolute loss.

The distinction between absolute and proportional loss is central to interpreting Table 3 and Figure 3. The very high correlation between polygon area and absolute loss is not surprising: a larger polygon contains more 30 m pixels and therefore has more opportunity to intersect a loss pixel. The coefficient of $\rho = 0.901$ should consequently not be presented as evidence that larger disasters were produced by greater forest loss. It is instead a strong reminder that spatial extent mechanically structures overlap statistics. Any causal study would need to move beyond this geometric relationship by defining contributing catchments and controlling for rainfall, topography, drainage density, soil properties, and exposure.

The weaker correlation between polygon area and proportional loss ($\rho = 0.364$) contains different information. It suggests that larger polygons tend, only modestly, to have higher loss relative to their own baseline, and the relationship explains far less of the rank ordering than the absolute-loss comparison. At the same time, the Kruskal–Wallis result ($H = 3.19$, $p = 0.203$) indicates that the available data do not support a statistically significant difference in proportional loss among flood, landslide, and landslide-area classes. This result argues against claiming a distinctive forest-loss signature for any of the three mapped classes within the current sample.

Individual polygons illustrate why summaries must be interpreted with scale and context. West Pasaman's flood polygon records 28.85% loss of baseline tree cover, while the Agam flood polygon records 19.24%. In Aceh, the Subulussalam landslide-area polygon records 24.55%, whereas Aceh Tamiang's large flood polygon records 20.20%. South Tapanuli contains a very small mapped landslide polygon with 34.11% proportional loss, demonstrating how a high percentage can arise within a small footprint. These values are useful for prioritization, but they are not directly comparable indicators of hydrological effect because the polygons differ greatly in area, geomorphic setting, baseline tree cover, and relationship to upstream contributing zones.

For floods in particular, loss measured inside the inundation polygon may be hydrologically downstream of the land-cover changes that matter most for runoff generation. A flooded lowland footprint can contain agricultural or urban land with relatively little baseline tree cover, while important disturbance may lie upstream outside the mapped inundation. Conversely, tree-cover loss inside a flood polygon may reflect floodplain or plantation dynamics that have little effect on peak discharge from the contributing catchment. This spatial mismatch is why the present analysis uses the overlap as a risk-screening signal rather than a watershed-process metric.

A practical next step is therefore to convert the polygon analysis into a nested catchment design. Each flood and landslide location could be linked to the relevant sub-watershed, after which pre-event loss could be summarized by upstream distance, slope class, legal forest function, and riparian position. Rainfall and discharge data could then be added to test whether catchments with different disturbance histories responded differently under comparable meteorological forcing. Process-informed or transferable machine-learning frameworks may be useful at that stage, provided that physically meaningful predictors and event validation are retained (Pakdehi et al., 2024).

3.4 Tree-cover loss within legally established forest areas

Across the legally established forest polygons, Protection Forest contained 92,564 ha of tree-cover loss and conservation areas contained 39,439 ha. Together, these protected functions contained 132,003 ha (1,320.03 km^2), equivalent to 3.10% of their summed tree-cover baseline. Production-forest functions contained 145,524 ha of loss (10.71% of baseline). The production-forest loss rate exceeded the combined protected-function rate, but non-zero loss inside Protection Forest and conservation areas confirms that legal designation does not by itself eliminate canopy disturbance.

Table 4. Tree-cover loss by province and broad legal forest function, 2014–2024

Province	Forest function	Source polygons	Tree-cover baseline (ha)	Loss (ha)	Loss (km^2)	Loss (%)
Aceh	Protection Forest	15	1,234.033	20,934	209.34	1.70
Aceh	Conservation Area	13	766,307	11,178	111.78	1.46
Aceh	Production Forest	12	262,188	13,669	136.69	5.21
North Sumatra	Protection Forest	36	668,498	37,331	373.31	5.58
North Sumatra	Conservation Area	28	356,716	5,738	57.38	1.61
North Sumatra	Production Forest	60	750,696	73,718	737.18	9.82
West Sumatra	Protection Forest	37	687,773	34,299	342.99	4.99
West Sumatra	Conservation Area	29	538,274	22,523	225.23	4.18
West Sumatra	Production Forest	59	345,738	58,138	581.38	16.82

(BIG One Map Forest-Estate Designation (*Penetapan Kawasan Hutan*) and Hansen Global Forest Change, processed by the author)

The legal-status overlay provides an empirical basis for assessing tree-cover loss across legally established forest functions. However, the analysis remains a spatial audit rather than an evaluation of individual permits or illegal activity. Hansen detects canopy loss from multiple causes, including harvest, plantation rotation, fire, storm damage, and permanent conversion. Consequently, the protected-area results justify targeted monitoring and investigation, not an automatic allegation of unlawful deforestation.

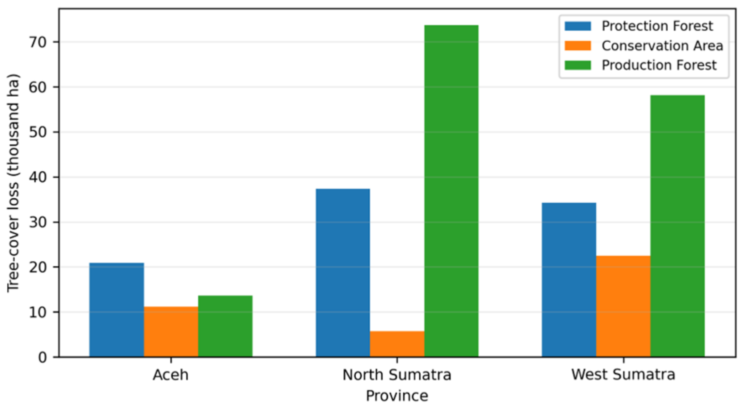

Fig. 4. Tree-cover loss within legally established forest functions by province, 2014–2024. (Author's analysis based on BIG One Map and Hansen Global Forest Change data)

The forest-function comparison adds information that cannot be inferred from the disaster polygons alone. Relative to their year-2000 tree-cover baselines, production-forest functions show a substantially higher combined loss rate than Protection Forest and conservation functions. That contrast is directionally consistent with the different management purposes of these legal categories, but it is not a direct measure of compliance or management performance. Hansen records canopy removal regardless of whether a change was authorized, temporary, accidental, or permanent, and the denominator remains baseline tree cover rather than total legal-area extent.

Provincial differences within the legal categories are also informative. Aceh shows relatively low proportional loss in Protection Forest (1.70%) and conservation areas (1.46%) compared with North Sumatra and West Sumatra. North Sumatra records 5.58% in Protection Forest and 1.61% in conservation areas, while West Sumatra records 4.99% and 4.18%, respectively. Production-forest loss is highest proportionally in West Sumatra at 16.82%, compared with 9.82% in North Sumatra and 5.21% in Aceh. These contrasts are screening signals that can guide more detailed examination of where and when canopy changes occurred inside particular legal units.

Indonesia provides a particularly relevant setting for distinguishing legal designation from observed landscape condition. Research has linked deforestation outcomes to political and administrative incentives (Burgess et al., 2012), while broader Southeast Asian scholarship shows that formal territorial categories interact with competing claims and powers of exclusion over land (Hall et al., 2011; Peluso & Lund, 2011). The present data cannot determine whether these mechanisms explain any specific loss pixel. They do, however, show where legal forest status and observed canopy change coexist spatially, creating a defensible basis for targeted follow-up rather than generalized allegations.

Such follow-up should proceed at the source-polygon level. A monitoring agency could first identify recent loss clusters within Protection Forest and conservation polygons, then compare them with official management boundaries, concession or permit records where applicable, fire history, plantation rotation, and very-high-resolution imagery. Field verification would be required where remote sensing cannot distinguish harvest, storm damage, fire, or permanent conversion. This staged approach preserves the strength of satellite screening—consistent coverage over large areas—while recognizing that legal interpretation requires evidence beyond a canopy-loss raster.

The forest-estate overlay becomes hydrologically informative when it is combined with watershed position rather than interpreted from legal category alone. Protection and conservation designations establish legal management objectives, but they do not mean that every hectare contributes equally to runoff regulation, slope stability, or sediment control. Hydrological relevance depends on position within a catchment, slope, soil, riparian connectivity, antecedent condition, and the type of disturbance. A future priority map should therefore combine legal forest function with hydrological position, rather than treating all loss pixels within a given legal category as equivalent.

3.5 Implications for disaster-risk reduction and spatial governance

The combined results support a narrower and more operational definition of politicized hydrology. The term does not mean that institutions replace physical hydrology; rather, institutions influence where ecological functions are retained, where settlements and infrastructure develop, and whether monitoring follows watershed boundaries. The evidence shows three spatially differentiated screening profiles: extensive flood footprints in Aceh, mixed flood–slope mapped classes in North Sumatra, and smaller mapped footprints in West Sumatra. It also identifies measurable antecedent tree-cover loss in the disaster-affected polygons and within legally established forest functions.

For risk management, the immediate technological implication is to link the BIG spatial inventory with routine remote-sensing monitoring and watershed-based screening. A practical monitoring system should flag new tree-cover loss in upstream Protection Forest and conservation areas, intersect these alerts with sub-watershed boundaries, and prioritize field verification where mapped flood or landslide footprints and landslide-area polygons indicate a need for closer assessment. This approach would complement, rather than replace, rainfall thresholds, river gauges, slope monitoring, Sentinel-1 flood mapping, and physically based or machine-learning susceptibility models.

The governance mechanism is most concrete at jurisdictional boundaries. Watersheds can connect upstream land-management decisions in one administrative unit with downstream exposure in another, while forest management, spatial planning, river management, disaster response, and infrastructure investment may be divided among different institutions. This creates an institutional-fit problem: ecological processes operate along catchments, but authority and information are often organized by sector and administrative territory. Work on social-ecological governance emphasizes that management is more effective when institutional arrangements fit the spatial and temporal scale of the processes being managed (Ostrom, 2009; Biermann et al., 2012). In this study, politicized hydrology therefore points to a testable coordination problem—whether cross-boundary environmental change and downstream risk are jointly monitored and acted upon—rather than to a claim that political factors replace physical hydrology.

The most immediate application is a tiered monitoring architecture. At the first tier, BIG disaster-affected polygons, annual Hansen or comparable tree-cover alerts, and official forest-function maps can be integrated to identify locations where mapped disaster areas coincide with notable landscape change. At the second tier, these locations can be linked to sub-watershed boundaries, slope and elevation, drainage networks, rainfall, and Sentinel-1 flood observations to test whether the spatial signal is hydrologically plausible. At the third tier, field observations, river-gauge records, land-management histories, and relevant planning or licensing documents can be used to evaluate mechanisms and responsibility. Each tier answers a different question and prevents a screening map from being mistaken for causal or legal proof.

For Aceh, the scale of the mapped flood footprint suggests that monitoring should prioritize large river corridors and the upstream areas contributing to North Aceh, East Aceh, and Aceh Tamiang. The purpose would not be to attribute the floods to forest loss, but to determine whether catchments feeding the largest inundation areas also contain concentrated recent disturbance, sediment-source zones, or loss within legally protected functions. Floodplain exposure, channel capacity, and rainfall must be examined simultaneously. This approach is more actionable than a province-wide statement that deforestation increases flooding because it identifies a testable sequence from screening to watershed diagnosis.

North Sumatra requires a somewhat different emphasis because the inventory includes both large flood polygons and substantial slope-related polygons. Central and South Tapanuli are logical priorities for integrated analysis of slope instability, sediment connectivity, and downstream flood exposure. Langkat, with the province's largest mapped flood polygon, is a priority for upstream–downstream catchment assessment. The forest-function results further indicate that Protection Forest in North Sumatra experienced a higher proportional loss than the equivalent category in Aceh, which strengthens the case for targeted monitoring without establishing a causal link to a particular disaster.

West Sumatra's smaller total disaster footprint should not result in a lower analytical priority. Its steep mountain-to-coast transitions can produce short response times, while the forest-function overlay shows comparatively high proportional loss in both Protection Forest and conservation areas and the highest proportional loss in production forests among the three provinces. West Pasaman and Agam also contain flood polygons with relatively high proportional loss. These observations support a strategy focused on rapid-response catchments, slope and riparian connectivity, and the spatial relationship between recent canopy change and settlements in narrow valleys or coastal plains.

The policy implication is therefore not a generic call for “more forest” or for uniform restrictions across all mapped areas. Effective risk reduction requires identifying which land-cover changes occur in hydrologically sensitive positions, which downstream assets are exposed, and which institution has authority to act. Land-use governance research shows that policy instruments can interact synergistically or undermine one another depending on design and implementation (Lambin et al., 2014). A watershed-based workflow can make those interactions more visible by connecting legal land status with measurable environmental change and downstream risk.

The study also suggests a clear evidentiary boundary for public communication and enforcement. A tree-cover-loss alert within a Protection Forest indicates that canopy removal occurred at the mapped pixel and time interval; it is not, by itself, evidence of an illegal act. A statistical association between polygon area and loss is evidence of spatial co-location; it is not evidence that the loss caused the hazard. A mapped flood or landslide polygon indicates an image-interpreted affected area, while the BIG Area Longsor class indicates an area in which several landslide occurrences were mapped. None of these geometries is a complete measure of social vulnerability or disaster impact. Maintaining these distinctions is essential if geospatial evidence is to support credible environmental governance rather than overextended claims.

4. Conclusions

This study provides a reproducible spatial screening of 65 hydrometeorological disaster-affected polygons in Aceh, North Sumatra, and West Sumatra. Flood polygons dominate the mapped area, while Hansen data show substantial regional tree-cover loss during 2014–2024 and measurable overlap with the disaster polygons. Tree-cover loss was also detected within legally established Protection Forests and conservation areas. The strong association between polygon size and absolute loss mainly reflects spatial scale, whereas proportional loss did not differ significantly among the three BIG classes. The results therefore establish co-location and screening priorities, not direct causation or a complete measure of disaster risk. The contribution of politicized hydrology in this study is to connect three evidence domains without collapsing them into one another: mapped hydrometeorological disaster areas, antecedent tree-cover change, and formal forest-estate governance. The analysis does not include event rainfall, terrain-based routing, population or asset exposure, or permit-level investigation; consequently, it cannot identify the complete causal chain of a specific disaster or determine the legality of a specific loss pixel. Those boundaries are part of the analytical design and define what the screening results can legitimately support.

The next analytical step is to move from mapped footprints to contributing catchments and add event-specific rainfall, terrain, drainage, sediment connectivity, exposure, and time-specific land-change information. A tiered workflow can first use national datasets to flag locations, then test hydrological plausibility at sub-watershed scale, and finally use high-resolution imagery, management records, and field verification where questions of mechanism, planning, licensing, or enforcement arise. In this form, politicized hydrology functions as a transparent bridge from reproducible geospatial screening to more rigorous hydrological and governance investigation. Operationally, the existing workflow can prioritize catchments where large mapped footprints, high proportional pre-event tree-cover loss, and loss within legally protected forest functions coincide. Such locations should be treated as candidates for further assessment rather than as proof of causation or non-compliance. This distinction preserves the practical value of the screening workflow while keeping the evidentiary claims consistent with the data and methods used.

Acknowledgement

The author would like to thank the Geospatial Information Agency (*Badan Informasi Geospasial*/BIG) for providing open access to the spatial datasets used in this study, and Universitas Indonesia for the academic support extended during the completion of this research.

Author Contribution

The author confirms sole responsibility for the following: study conception and design, data collection, analysis and interpretation of results, and manuscript preparation. The author reviewed and approved the final version of the manuscript.

Funding

This research received no external funding.

Ethical Review Board Statement

Not available.

Informed Consent Statement

Not available.

Data Availability Statement

The data supporting the findings of this study are publicly available from online databases. The disaster-polygon dataset is distributed by the Geospatial Information Agency, while Hansen Global Forest Change data are available through Google Earth Engine. The datasets can be accessed at: https://bit.ly/4gBozj2. The processed tabular outputs and analysis scripts are available from the corresponding author upon reasonable request.

Conflicts of Interest

The authors declare no conflict of interest.

Declaration of Generative AI Use

During the preparation of this work, the author used Grammarly to assist in improving the manuscript's grammar, clarity, and academic tone. After using this tool, the author reviewed and edited the content as needed and took full responsibility for the publication's content.

References

Abood, S. A., Lee, J. S. H., Burivalova, Z., Garcia-Ulloa, J., & Koh, L. P. (2015). Relative contributions of the logging, fiber, oil palm, and mining industries to forest loss in Indonesia. *Conservation Letters, 8*(1), 58–67. https://doi.org/10.1111/conl.12103

Austin, K. G., Mosnier, A., Pirker, J., McCallum, I., Fritz, S., & Kasibhatla, P. S. (2017). Shifting patterns of oil palm driven deforestation in Indonesia and implications for zero-deforestation commitments. *Land Use Policy, 69*, 41–48. https://doi.org/10.1016/j.landusepol.2017.08.036

Austin, K. G., Schwantes, A., Gu, Y., & Kasibhatla, P. S. (2019). What causes deforestation in Indonesia? *Environmental Research Letters, 14*(2), 024007. https://doi.org/10.1088/1748-9326/aaf6db

Avand, M., Moradi, H., & Ramazanzadeh Lasboyee, M. (2021). Using machine learning models, remote sensing, and GIS to investigate the effects of changing climates and land uses on flood probability. *Journal of Hydrology, 595*, 125663. https://doi.org/10.1016/j.jhydrol.2020.125663

Badan Informasi Geospasial. (2024). *Penetapan kawasan hutan [Feature layer]*. Kebijakan Satu Peta, Service PUBLIK/KEHUTANAN, Layer 0. https://kspservices.big.go.id/satupeta/rest/services/PUBLIK/KEHUTANAN/MapServer/0

Badan Informasi Geospasial. (2026). *Peta area terdampak bencana hidrometeorologi: Aceh, Sumatera Utara, dan Sumatera Barat* [Spatial dataset and metadata]. Ina-Geoportal data download. https://tanahair.indonesia.go.id/portal-web/unduh

Biermann, F., Abbott, K., Andresen, S., Bäckstrand, K., Bernstein, S., Betsill, M. M., Bulkeley, H., Cashore, B., Clapp, J., Folke, C., Gupta, A., Gupta, J., Haas, P. M., Jordan, A., Kanie, N., Kluvánková-Oravská, T., Lebel, L., Liverman, D., Meadowcroft, J., ... Zondervan, R. (2012). Navigating the Anthropocene: Improving Earth system governance. *Science, 335*(6074), 1306–1307. https://doi.org/10.1126/science.1217255

Bradshaw, C. J. A., Sodhi, N. S., Peh, K. S.-H., & Brook, B. W. (2007). Global evidence that deforestation amplifies flood risk and severity in the developing world. *Global Change Biology, 13*(11), 2379–2395. https://doi.org/10.1111/j.1365-2486.2007.01446.x

Bruijnzeel, L. A. (2004). Hydrological functions of tropical forests: Not seeing the soil for the trees? *Agriculture, Ecosystems & Environment, 104*(1), 185–228. https://doi.org/10.1016/j.agee.2004.01.015

Burgess, R., Hansen, M., Olken, B. A., Potapov, P., & Sieber, S. (2012). The political economy of deforestation in the tropics. *The Quarterly Journal of Economics, 127*(4), 1707–1754. https://doi.org/10.1093/qje/qjs034

Gaveau, D. L. A., Locatelli, B., Salim, M. A., Husnayaen, Manurung, T., Descals, A., Angelsen, A., M., E., & Sheil, D. (2022). Slowing deforestation in Indonesia follows declining oil palm expansion and lower oil prices. *PLoS ONE, 17*(3), e0266178. https://doi.org/10.1371/journal.pone.0266178

Hall, D., Hirsch, P., & Li, T. M. (2011). *Powers of exclusion: Land dilemmas in Southeast Asia*. NUS Press. https://nuspress.nus.edu.sg/products/powers-of-exclusion

Hansen, M. C., Potapov, P. V., Moore, R., Hancher, M., Turubanova, S. A., Tyukavina, A., Thau, D., Stehman, S. V., Goetz, S. J., Loveland, T. R., Kommareddy, A., Egorov, A., Chini, L., Justice, C. O., & Townshend, J. R. G. (2013). High-resolution global maps of 21st-century forest cover change. *Science, 342*(6160), 850–853. https://doi.org/10.1126/science.1244693

Islam, T., Zeleke, E. B., Afroz, M., & Melesse, A. M. (2025). A systematic review of urban flood susceptibility mapping: Remote sensing, machine learning, and other modeling approaches. *Remote Sensing, 17*(3), 524. https://doi.org/10.3390/rs17030524

Kelly, A. B., & Peluso, N. L. (2015). Frontiers of commodification: State lands and their formalization. *Society & Natural Resources, 28*(5), 473–495. https://doi.org/10.1080/08941920.2015.1014602

Lambin, E. F., & Meyfroidt, P. (2011). Global land use change, economic globalization, and the looming land scarcity. *Proceedings of the National Academy of Sciences, 108*(9), 3465–3472. https://doi.org/10.1073/pnas.1100480108

Lambin, E. F., Meyfroidt, P., Rueda, X., Blackman, A., Börner, J., Cerutti, P. O., Dietsch, T., Jungmann, L., Lamarque, P., Lister, J., Walker, N. F., & Wunder, S. (2014). Effectiveness and synergies of policy instruments for land use governance in tropical regions. *Global Environmental Change, 28*, 129–140. https://doi.org/10.1016/j.gloenvcha.2014.06.007

Lemos, M. C., & Agrawal, A. (2006). Environmental governance. *Annual Review of Environment and Resources, 31*, 297–325. https://doi.org/10.1146/annurev.energy.31.042605.135621

Ostrom, E. (2009). A general framework for analyzing sustainability of social-ecological systems. *Science, 325*(5939), 419–422. https://doi.org/10.1126/science.1172133

Pakdehi, M., Ahmadisharaf, E., Nazari, B., & Cho, E. (2024). Transferability of machine-learning-based modeling frameworks across flood events for hindcasting maximum river water depths in coastal watersheds. *Natural Hazards and Earth System Sciences, 24*, 3537–3559. https://doi.org/10.5194/nhess-24-3537-2024

Peluso, N. L., & Lund, C. (2011). New frontiers of land control: Introduction. *The Journal of Peasant Studies, 38*(4), 667–681. https://doi.org/10.1080/03066150.2011.607692

Robbins, P. (2012). *Political ecology: A critical introduction* (2nd ed.). Wiley-Blackwell. https://books.google.com/books?id=NixJcZnSsv8C

Syvitski, J. P. M., Vörösmarty, C. J., Kettner, A. J., & Green, P. (2005). Impact of humans on the flux of terrestrial sediment to the global coastal ocean. *Science, 308*(5720), 376–380. https://doi.org/10.1126/science.1109454

Tan-Soo, J.-S., Adnan, N., Ahmad, I., Pattanayak, S. K., & Vincent, J. R. (2016). Econometric evidence on forest ecosystem services: Deforestation and flooding in Malaysia. *Environmental and Resource Economics, 63*(1), 25–44. https://doi.org/10.1007/s10640-014-9834-4

Tarigan, S. D. (2016). Land cover change and its impact on flooding frequency of Batanghari Watershed, Jambi Province, Indonesia. *Procedia Environmental Sciences, 33*, 386–392. https://doi.org/10.1016/j.proenv.2016.03.089

Wells, J. A., Wilson, K. A., Abram, N. K., Nunn, M., Gaveau, D. L. A., Runting, R. K., Tarniati, N., Mengersen, K. L., & Meijaard, E. (2016). Rising floodwaters: Mapping impacts and perceptions of flooding in Indonesian Borneo. *Environmental Research Letters, 11*(6), 064016. https://doi.org/10.1088/1748-9326/11/6/064016

Wheater, H., & Evans, E. (2009). Land use, water management and future flood risk. *Land Use Policy, 26*, S251–S264. https://doi.org/10.1016/j.landusepol.2009.08.019

Young, O. R. (2017). *Governing complex systems: Social capital for the Anthropocene*. MIT Press. https://doi.org/10.7551/mitpress/9780262035934.001.0001

Biography of Author

Miftahul Ardli, Department of Environmental Science, Graduate School of Sustainable Development, Universitas Indonesia, Central Jakarta, Special Capital Region of Jakarta 10430, Indonesia.

- Email: mifardli21@gmail.com
- ORCID: N/A
- Web of Science ResearcherID: N/A
- Scopus Author ID: N/A
- Homepage: N/A